A Myosin Head Can Interact with Two Chemically Modified G-Actin Monomers at ATP-Modulated Multiple Sites†

Toshiaki Arata*

Department of Biology, Graduate School of Science, Osaka University, Toyonaka, Osaka 560, Japan

Received April 3, 1996; Revised Manuscript Received October 9, 1996⊗

ABSTRACT: It has been reported that chemically modified [with *m*-maleimidobenzoic acid *N*-hydroxysuccinimide ester (MBS)] actin maintains its monomeric form and retains the ability to bind (and make chemical cross-links) to myosin head [Bettache, N., Bertrand, R., & Kassab, R. (1989) *Proc. Natl. Acad. Sci. U.S.A. 86*, 6028−6032; Arata, T. (1991) *J. Biochem. (Tokyo) 109*, 335−340]. Here, the interaction between MBS-G-actin and myosin subfragment 1 (S1) has been further studied by proteolytic susceptibility and chemical cross-linking. Two moles of MBS-actin monomers bound to 1 mol of myosin heads or S1 with different affinities. The first binding of MBS-G-actin to S1 strongly protected a 27-kDa/50-kDa junction of S1 heavy chain from trypsin digestion and also weakly protected a 50-kDa/20-kDa junction. The second binding protected a 50-kDa/20-kDa junction more strongly. ATP weakened these bindings more than 10-fold. MBS-G-actin was cross-linked to S1 by 1-ethyl-3-[3-(dimethylamino)propyl]-carbodiimide, producing the 175−185-kDa doublet bands similar to those of F-actin and S1. The first binding produced a complex migrating at 175 kDa on gels [Hozumi, T. (1992) *Biochemistry 31*, 10071−10073] and the second binding further produced an 185-kDa complex, suggesting that two binding sites correspond to two spatially separated cross-linking sites. MBS-G-actin was also cross-linked by MBS to S1 when the first actin binds, producing only 180-kDa complex. In the presence of ATP or ADP, an 140-kDa complex was produced together with the 180-kDa complex, suggesting shifting of the binding site.

Muscle contraction results from the sliding of the thick (myosin-containing) filaments past the thin (actin-containing) filaments (Huxley & Niedergerke, 1954; Huxley & Hanson, 1954). The sliding force or motion is generated by cyclic interaction of myosin heads with F-actin. This interaction is coupled to ATP hydrolysis and may involve translocation of multiple binding sites between myosin head (S1)[1] and actin. Recently, atomic structures of three-dimensional crystals of actin and myosin head have been elucidated. It is therefore very important to know the position of actin binding sites on myosin heads. Chemical cross-linking and proteolytic studies suggest that there are multiple binding sites between myosin subfragment 1 (S1) and F-actin (Mornet et al., 1979, 1981; Sutoh, 1983; Arata, 1986; Yamamoto, 1990; dos Remedios & Moens, 1995).

It was shown that polymerization of G-actin induced by salts is greatly suppressed by reaction of G-actin with *m*-maleimidobenzoic acid *N*-hydroxysuccinimide ester (MBS). This polymerization-resistant MBS-actin retained the ability to bind to myosin head and dissociate in the presence of ATP (Bettache et al., 1989; Arata, 1991). Chaussepied and Kasprzak (1989a) also found that G-actin did not polymerize and formed a 1:1 complex with S1 containing only a light chain 3. Recently, Heintz and Faulstich (1996) found that G-actin cross-linked between Cys374 and Cys10 did not polymerize but still bound to S1. The previous study on MBS-actin showed that two MBS-actin monomers bind to a myosin head (Arata, 1991). The latter result agreed well with Valentin-Ranc et al. (1991), who used a pyridoxal phosphate-modified actin monomer. When these modified actin monomers were cross-linked to S1 by EDC at 1:1 molar ratio, only the lower-mass species of two products found in the F-actin−S1 system (migrating at 175 and 185 kDa on SDS−polyacrylamide gels) was yielded (Hozumi, 1992; Combeau et al., 1992). Andreeva et al. (1993) and later Bonafe and Chaussepied (1995) found that two actin protomers of F-actin were chemically cross-linked to a single S1. In the present study, tryptic digestion with various molar ratios of S1 and MBS-G-actin demonstrated that the binding of two MBS-G-actins to S1 protects 27-kDa/50-kDa and 20-kDa/50-kDa tryptic-cleavable junctions of S1 heavy chain with different affinities, suggesting two separate binding sites for monomeric actin. EDC cross-linking experiments with various molar ratios of S1 and MBS-G-actin suggested that 175−185-kDa doublet bands correspond to two distinct complexes formed through two separate binding sites. We also studied MBS cross-linking between monomeric MBS-actin and S1 in the presence of ATP and found that a new covalent complex appeared on gels at 140 kDa together with the 180-kDa species that exists in the absence of ATP, suggesting actin binding site shifting. Characterization of the binding nature of this actin will be helpful for studying the location of the binding sites by electron microscopy or

† This study was supported in part by Grants-in-Aid for Scientific Research (04680269) and for Scientific Research on Priority Areas (05244208, 06235209, and 07224206) from the Ministry of Education, Science, Sports and Culture of Japan.

* Phone: 81-6-850-5427. FAX: 81-6-850-5441. E-mail: arata@bio.sci.osaka-u.ac.jp.

⊗ Abstract published in *Advance ACS Abstracts*, November 15, 1996.

[1] Abbreviations: S1, myosin subfragment 1; MBS, *m*-maleimidobenzoic acid *N*-hydroxysuccinimide ester; EDC, 1-ethyl-3-[3-(dimethylamino)propyl]carbodiimide; IAEDANS, 5-[[2-[(iodoacetyl)amino]ethylamino]naphthalene-1-sulfonic acid; SDS, sodium dodecyl sulfate.

S0006-2960(96)00803-3 CCC: $12.00

for studying the tertiary structure of acto−S1 complex by X-ray crystallography.

Some aspects of this work have already been described in abstract form (Arata, 1993, 1995).

MATERIALS AND METHODS

Chemicals. MBS was purchased from Sigma Chemical Co. and EDC was from Nacalai Tesque, Japan. 9-Anthroylnitrile was purchased from Wako Pure Chemicals Co., Japan. Sephadex G-25 was purchased from Pharmacia. L-1-(Tosylamido)-2-phenylethyl chloromethyl ketone-treated trypsin was obtained from Worthington Biochemical Co. Trypsin inhibitor (from chicken egg white) was from Sigma Chemical Co.

Proteins. Myosin was prepared from rabbit white muscle as described by Perry (1955). S1 was obtained by α-chymotryptic digestion according to Weeds and Taylor (1975). S1 was modified at Cys707 (SH1) with IAEDANS (Arata, 1986) and at the N-terminal 27-kDa fragment with 9-anthroylnitrile (Hiratsuka, 1989). Actin was prepared as described by Spudich and Watt (1971).

Monomeric actin was prepared by mixing G-actin (∼2 mg/mL) with 1−3 mM MBS (dissolved at 100 mM in dimethylformamide) in a conventional depolymerizing buffer (10 mM triethanolamine and 10−20 μM ATP at pH 8.0) for 1−2 h at 20 °C. The reaction was terminated by the addition of 25 mM 2-mercaptoethanol and 60 mM monoethanolamine. After the mixture was centrifuged at 520000*g* for 30 min in the presence of 0.1 M KCl, the actin in the supernatant was gel-filtered over a Sephadex G-25 column equilibrated by a conventional depolymerization buffer without ATP (10 mM triethanolamine at pH 8.0). To avoid protein denaturation, the MBS-actin in the ATP-free buffer was immediately used for experiments. For MBS cross-linking experiments, MBS-actin was not treated with 2-mercaptoethanol and monoethanolamine. MBS-F-actin and native F-actin were obtained by resuspending the pellet in 10 mM triethanolamine (pH 8.0) and 2 mM $MgCl_2$ after MBS-G-actin or native G-actin was polymerized by 30-min incubation with a 2-fold molar excess of phalloidin, 10 mM KCl, and 5 mM $MgCl_2$ at 20 °C and centrifuged at 120000*g*.

Protein concentrations were determined by the biuret method. The method of Bradford (1976) was also used to measure the concentrations of proteins by a calibration of the respective proteins as standards.

Methods. The binding of monomeric MBS-actin to myosin filaments was determined by measuring the protein concentration in the supernatant after the reaction mixture was centrifuged at 130000*g* for 10 min (Arata, 1991).

Trypsin digestion of S1 (5 μM) was performed in the presence of MBS-actin at a weight ratio of 1:50 (trypsin:S1) for 30 min at 20 °C in 0.5 mM $MgCl_2$ and 10 mM triethanolamine (pH 8.0) unless otherwise stated. The digestion was terminated by the addition of egg trypsin inhibitor (2-fold excess).

MBS cross-linking experiments were performed as follows: Native S1 or modified S1 (5 μM) was mixed with MBS-G-actin (not treated with 2-mercaptoethanol and monoethanolamine) at 20 °C in 0.5 mM $MgCl_2$ and 10 mM triethanolamine (pH 8.0) unless otherwise stated. After 30 min, the reaction was terminated by the addition of 2.5 mM dithiothreitol. EDC cross-linking experiments were performed for 30 min in the presence of 15 mM EDC under the same conditions except that MBS-G-actin had been quenched.

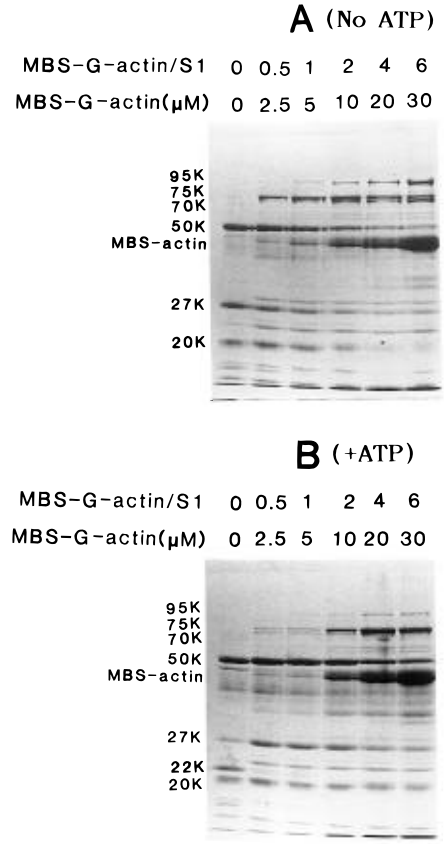

FIGURE 1: Electrophoretic patterns of tryptic digestion of S1 in the presence of MBS-G-actin. Tryptic digestion of S1 (5 μM) was performed in the presence of 2.5−30 μM MBS-G-actin at a weight ratio of 1:50 (trypsin:S1) for 30 min at 20 °C in 0.5 mM $MgCl_2$ and 20 mM triethanolamine (pH 8.0). MgATP (1 mM) was absent in (A) and present in (B). On the top of the figure, MBS-G-actin concentration (micromolar) and MBS-G-actin:S1 molar ratio are indicated.

The Mg-dependent ATPase activity was measured in 0.5 mM ATP, 0.2 mg/mL pyruvate kinase, 2 mM $MgCl_2$, 2 mM phosphoenolpyruvate, and 6 mM KCl at pH 7.0 and 20 °C. The amount of pyruvate liberated was assayed by the method of Reynard et al. (1961).

SDS−polyacrylamide slab gel electrophoresis (7.5% or 12.5% acrylamide) was performed using a buffer system of Laemmli (1970). Gels were stained by Coomassie brilliant blue. Band intensity was measured using a Fuji-Riken densitometer FD-A4.

RESULTS

Tryptic Digestion of S1 Bound to MBS-G-Actin. S1 is split into three fragments of 27, 50, and 20 kDa by limited tryptic digestion. F-actin binding to S1 strongly protects a 50-kDa/20-kDa junction and abolishes the production of the 20-kDa fragment. However, MBS-G-actin protects a 27-kDa/50-kDa junction but not the 50-kDa/20-kDa junction (Bettache et al., 1989; Hozumi, 1992). Figure 1 shows the electrophoretic patterns of the tryptic digestion (digestion time = 30 min) of S1 in the presence of MBS-G-actin at different concentrations. In the absence of ATP, the 27-kDa band became weaker when MBS-G-actin was added to S1 at a molar ratio of about 1, consistent with the previous reports. However,

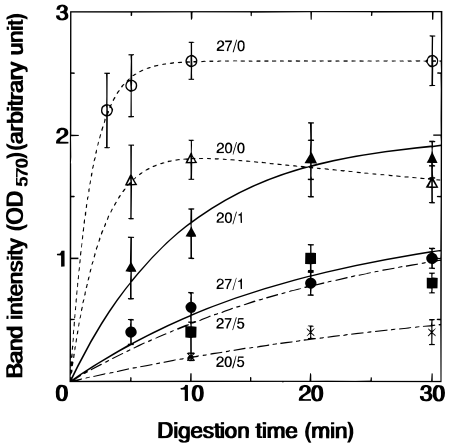

FIGURE 2: Time course of band intensities of 27-kDa (○, ●, ■) and 20-kDa (△, ▲, ×) fragments produced by tryptic digestion of S1 in the presence of MBS-G-actin at actin-to-S1 molar ratios of 0 (○, △), 1 (●, ▲), and 5 (■, ×). Tryptic digestion was performed as described in Figure 1, except that the digestion time was variable and MgATP was absent. The error bars indicate standard deviation of two or three measurements.

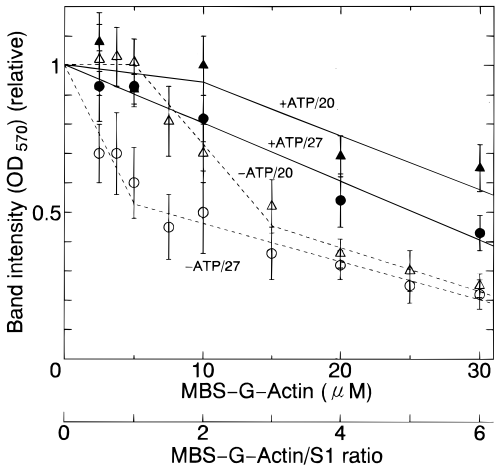

FIGURE 3: Band intensities of 27-kDa (○, ●) and 20-kDa (△, ▲) tryptic fragments as a function of MBS-G-actin concentration or MBS-G-actin:S1 molar ratio. Tryptic digestion was performed in the absence (○, △) or presence (●, ▲) of 1 mM MgATP, as described in Figure 1. The error bars indicate standard deviation of two or three measurements.

further addition of MBS-G-actin caused the 20-kDa band to become weaker and finally both 20- and 27-kDa bands became faint at ratios more than 2. In the presence of ATP, the 27-kDa fragment was degraded into the 22-kDa fragment (Hozumi, 1983). Addition of MBS-G-actin caused a small effect. The 20- and 27-kDa bands became weaker only at high concentrations of MBS-G-actin. It remained unclear why the degradation of 27-kDa fragment appeared to be suppressed almost completely at the molar ratio of 0.5. It is unlikely that ATP was rapidly converted to ADP, because ADP also degrades the 27-kDa fragment like ATP (Hozumi, 1983). It is probable that MBS-actin suppresses some steps of production and degradation of the 27-kDa fragment in binding equilibrium to reduce greatly the overall production rate of the 22-kDa fragment. Muhlrad and Hozumi (1982) reported that the 29.5-kDa to 27-kDa conversion also depends nonlinearly on ATP binding to S1.

To know the nature of MBS-G-actin protection, the kinetics of trypsin digestion was analyzed. Figure 2 shows the time course of changes in the 20- and 27-kDa band intensities. In the absence of MBS-actin, both 20- and 27-kDa bands appeared very fast within 5 min. When MBS-actin was present at an actin:S1 molar ratio of 1, the intensity of the 27-kDa band increased slowly to a third of the control (no MBS-G-actin) at 30 min. The production of the 20-kDa band also became slow; the intensity of the 20-kDa band increased slowly and reached to the control level (no MBS-actin) at 30 min. No inhibition was seen at a 30-min digestion time (see Figure 1). At a high molar ratio of 5, the production of the 27-kDa band was still slow as at the molar ratio of 1. On the other hand, the 20-kDa band production was suppressed; the intensity of the 20-kDa band increased very slowly to only a fourth of the control at 30 min. These results demonstrate that the 27-kDa/50-kDa junction was protected by MBS-G-actin at actin/S1 molar ratios ≥ 1, whereas the 50-kDa/20-kDa junction was weakly protected at a molar ratio of 1 and strongly protected at higher molar ratios.

Figure 3 shows the 20- and 27-kDa band intensities as a function of MBS-G-actin concentration. As shown in the original experiment of Figure 1, the band intensity of the 27-kDa fragment produced during a 30-min digestion decreased markedly to about half with increasing actin:S1 molar ratios up to about 1 and gradually decreased at higher ratios. On the other hand, the 20-kDa band intensity stayed at almost the original level at the molar ratio up to about 1 and decreased gradually to the steady-state level (about a third) at molar ratios of 2−4. However, the 20-kDa band intensity after a short 2-min digestion changed like the 27-kDa band intensity: it decreased markedly at a molar ratio of about 1 as expected from Figure 2 (data not shown). The presence of ATP weakened the effect of MBS-G-actin. Both the 20- and 27-kDa (+ 22-kDa) band intensities decreased gradually to only about half at high concentrations (30 μM) of MBS-actin. ADP did not change the effect of MBS-G-actin, although the 27-kDa band degraded into the 22-kDa band as in the presence of ATP (data not shown).

To know whether the protection of the two separate junctions is associated with the binding of two MBS-G-actin molecules, we compared the direct binding of MBS-G-actin to myosin heads and its protection of S1 proteolysis. Figure 4 shows the binding of MBS-G-actin to myosin heads of myosin filaments as a function of MBS-G-actin. The bound MBS-G-actin increased and reached about 2 mol/mol of myosin, as consistent with a previous report (Arata, 1991). ATP weakened the binding of MBS-G-actin. The binding curves were calculated as $(I_0 - I)/0.9$ from the protection of 27- and 20-kDa band production by assuming simply that two MBS-G-actin molecules can bind to two separate binding sites (27-kDa/50-kDa and 50-kDa/20-kDa junctional regions): each binding protects each junction by 90% from tryptic cleavage. I_0 and I represent the band intensities at zero and given concentrations of MBS-G-actin, respectively. The curves calculated for total binding compared with the direct binding data fairly well, although the calculated curve did not fit so well the binding data in the presence of ATP.

The binding curves for two sites in the absence of ATP could be simulated by the method of Valentin-Ranc et al. (1991) assuming sequential actin binding: S1 + MBS-G-actin $\rightleftarrows$ S1−MBS-G-actin + MBS-G-actin $\rightleftarrows$ S1−(MBS-G-actin)$_2$. We also tried to simulate the binding curves by assuming that actin can bind independently to either one of

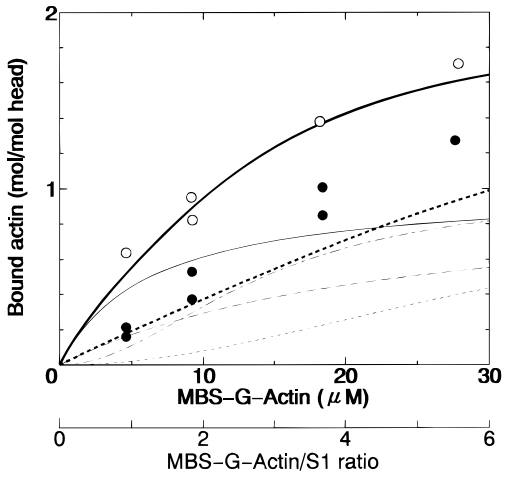

FIGURE 4: Binding of MBS-G-actin to myosin heads. The binding was directly measured by cosedimentation of MBS-G-actin with myosin filaments in the absence (○) or presence (●) of 1 mM MgATP (Arata, 1991). Continuous and dot-and-dash lines are the binding curves calculated as $(I_0 - I)/0.9$ from MBS-G-actin-induced decrease in the tryptic 20- and 27-kDa band intensities (shown in Figure 3), by assuming that two MBS-G-actin molecules can bind to two separate binding sites and prevent 20- and 27-kDa fragment production by 90%. I_0 and I represent band intensities at zero and given concentrations of MBS-G-actin, respectively. Two dashed lines are the binding curves calculated in the same way from the data in the presence of 1 mM MgATP. It should be noted that the direct binding is associated with the sum (thick line or thick dashed line) of the two binding curves calculated from tryptic digestion.

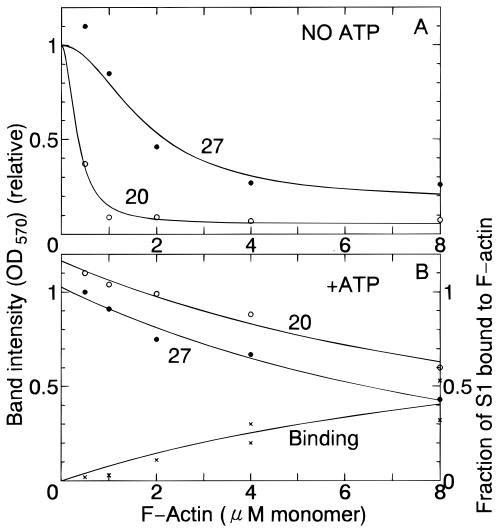

FIGURE 5: Tryptic digestion of F-actin−S1 complex in the absence (A) and presence (B) of ATP at various actin concentrations. Tryptic digestion of S1 (1 μM) was performed in the presence of phalloidin-polymerized F-actin (0.5-8 μM actin monomer) at trypsin:S1 weight ratio of 1:15 for 90 s in the absence and presence of 2.5 mM MgATP as described in Figure 1. Band intensities of tryptic 27-kDa (●) and 20-kDa (○) fragments are plotted as a function of actin concentration. Fraction of S1 bound to F-actin (×) in the presence of ATP are also plotted in the lower panel.

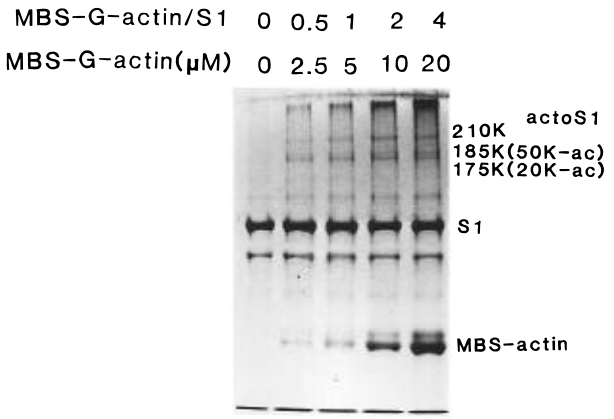

FIGURE 6: Chemical cross-linking of MBS-G-actin to S1 by EDC. Cross-linking was performed under the same conditions as trypsin digestion in the absence of ATP in Figure 1. MBS-G-actin (2.5−20 μM) was incubated with S1 (5 μM) for 30 min at 20 °C in 15 mM EDC, 0.5 mM $MgCl_2$, and 20 mM triethanolamine (pH 8.0). On the top of the figure, MBS-G-actin concentration (μM) and MBS-G-actin:S1 molar ratio are indicated. The doublet 175- and 185-kDa bands correspond to the acto−S1 complexes (20K-ac and 50K-ac) generated by cross-linking the 20- and 50-kDa domains of S1 to the N-terminal region of actin, respectively.

two binding sites with different affinities, protecting each tryptic junction. This independent binding model could not explain the very cooperative binding for the second site (data not shown): the first binding (1 mol) and almost no second binding occur at an 1:1 molar ratio (Figures 3 and 4). The dissociation constants for two binding sites were estimated separately from the protection curves obtained at lower S1 concentrations (data not shown). The dissociation constants for the first (27-kDa/50-kDa junction) and the second (50-kDa/20-kDa junction) binding were $(1-2) \times 10^{-6}$ M and $(4-5) \times 10^{-6}$ M, respectively. This 3−5-fold difference in two dissociation constants was essentially required to fit the data at high protein concentrations (Figure 4) by the sequential model (data not shown). At much higher S1 concentrations, this cooperative binding become clearer (data not shown). In the presence of ATP, the constants were $(2-3) \times 10^{-5}$ M.

Only the 50-kDa/20-kDa (not the 27-kDa/50-kDa) junction of S1 is known to be protected by F-actin from trypsin, although both are protected from V_8 protease or papain (Yamamoto, 1990; Lheureux & Chaussepied, 1995). However, we found that F-actin protected both junctions from trypsin at different actin:S1 molar ratios in the low-salt solution used for MBS-G-actin (Figure 5A). The intensity of the 20-kDa band produced in 90 s at a 1:15 molar ratio of trypsin decreased markedly at 1 μM actin (1:1 molar ratio) and stayed at the same level. On the other hand, the 27-kDa band intensity decreased markedly with increasing actin concentration higher than 1 μM and reached the steady-state level at 2−4 μM actin (ratio of 2−4). The same result was obtained under the standard proteolytic conditions (data not shown). ADP did not change the F-actin effect. However, at 0.1 M KCl the 27-kDa band did not weaken by F-actin (data not shown), as reported previously (Mornet et al., 1979). In the presence of ATP, the intensity of both bands decreased gradually with increasing actin concentration, as expected from weak binding (Figure 5B). This decrease was linearly correlated with the fraction of S1 bound to F-actin during ATP hydrolysis.

Cross-Linking Experiments. To examine the interface structure of MBS-G-actin−S1 and $(MBS\text{-}G\text{-}actin)_2$−S1 complexes in the presence and absence of ATP, we employed the chemical cross-linking of MBS-G-actin to S1 with EDC (Hozumi, 1992) and MBS itself (Bettache et al., 1989). Figure 6 shows the electrophoretic pattern of EDC cross-linking of MBS-G-actin to S1 under the same conditions used for tryptic digestion in the absence of ATP (Figure 1). A doublet band of 175−185 kDa apparent molecular weight was observed as for the F-actin−S1 system. A 175-kDa

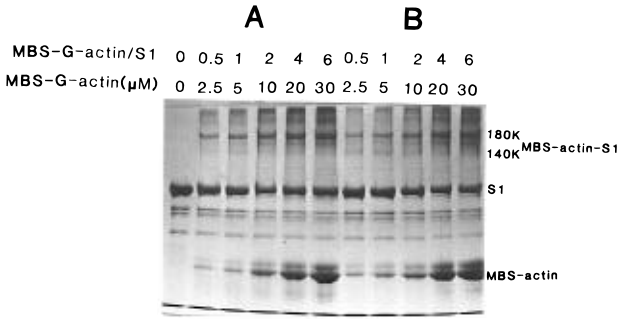

FIGURE 7: Chemical cross-linking of MBS-G-actin to S1 through reactive MBS of actin. Chemical cross-linking was performed under the same conditions as trypsin digestion in Figure 1. Reactive MBS-G-actin (2.5-30 μM) was incubated with S1 (5 μM) for 30 min at 20 °C in 0.5 mM $MgCl_2$ and 20 mM triethanolamine (pH 8.0). MgATP (1 mM) was absent in (A) and present in (B). Other conditions were described in Figure 6.

band was produced exclusively and the 185-kDa band was faint at an actin:S1 molar ratio of 1 (Hozumi, 1992). The intensity of the 185-kD band increased markedly at the higher molar ratios of 2−4 but was still less than that of the 175-kDa band. This agreed well with the finding, using the F-actin−S1 system, that the 175-kDa band appeared exclusively at a molar ratio of 1 and the 185-kDa band further appeared at higher ratios (Andreev & Borejdo, 1995). The 210-kDa band of actin−S1 product was also observed as reported by Combeau et al. (1992), using a monomeric actin modified with pyridoxal phosphate, and it became prominent at the higher molar ratios of 2−4. When S1 was labeled with IAEDANS at Cys707(SH1), the fluorescent 175-, 185-, and 210-kDa bands were seen (data not shown). When cross-linking experiments were done in the presence of ATP, these bands were very weak even at high ratios (data not shown) as with F-actin (Arata, 1986; Yamamoto, 1989). ADP had a small effect and somewhat (by about 30%) suppressed the production rates of these bands (data not shown).

Figure 7 shows the electrophoretic pattern of the cross-linking of MBS-G-actin to S1 by free MBS of MBS-G-actin under the same conditions as used for tryptic digestion (Figure 1). In the absence of ATP, an 180-kDa band was produced at an actin:S1 molar ratio of 1 as reported previously (Figure 7A). When S1 was labeled with IAEDANS at Cys707(SH1), a fluorescent 180-kDa band was seen (data not shown). However, any other band was not produced at the higher molar ratios where the second binding occurs.

In the presence of ATP, the 180-kDa band became weaker and appeared gradually with increasing MBS-G-actin concentration. A new 140-kDa band was produced together with the 180-kDa band (Figure 7B). The amount of 140-kDa band relative to 180-kDa band increased at pH 7.0 (data not shown). However, lowering the pH to 7.0 in the absence of ATP did not produce the 140-kDa band (data not shown). ADP has a similar effect to ATP (Figure 8B). The 180-kDa band appeared as strongly as in the absence of nucleotide. The cross-linked 180-kDa MBS-G-actin−S1 complex does not interact with native F-actin (Bettache et al., 1989). To see whether F-actin can bind to an 140-kDa cross-linked complex, we centrifuged the cross-linked MBS-G-actin−S1 solution mixed with F-actin. The 180-kDa band, produced in the absence of ATP, recovered in the supernatant and only a small fraction of it existed in the pellet (Figure

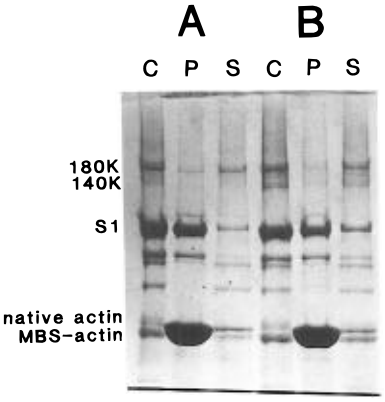

FIGURE 8: No F-actin binding to S1 chemically cross-linked to MBS-G-actin. S1 (20 μM) and reactive MBS-G-actin (16 μM MBS-actin) were cross-linked in the absence (A) and presence (B) of 1 mM MgADP and 10 μM diadenosine pentaphosphate (adenylate kinase inhibitor). Other conditions were described in Figure 7. MBS-actin−S1 mixture (C) was supplemented with a 4-fold molar excess of F-actin (stabilized by phalloidin). After sedimentation the supernatant (S) and pellet (P) were analyzed by SDS−polyacrylamide gels.

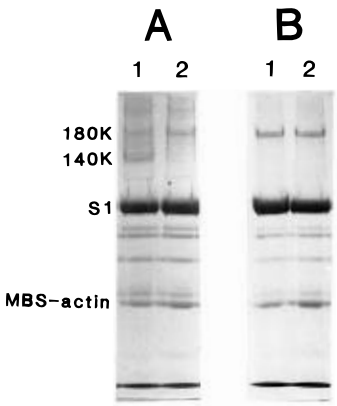

FIGURE 9: Inhibition of the ATP-induced 140-kDa band production by blocking SH1 of S1. Native S1 (lanes 1) or AEDANS-S1 (lanes 2) (12 μM) was cross-linked to MBS-G-actin (16 μM) in the presence (A) and absence (B) of ATP. Other conditions were as described in Figure 7.

8A), as consistent with the previous report. MBS-actin was cross-linked to S1 in the presence of ADP at an actin:S1 molar ratio of 0.8. The cross-linked solution was mixed with excess F-actin and then centrifuged. As shown in Figure 8B, the 140- and 180-kDa bands recovered in the supernatant and only a small fraction of them existed in the pellet, demonstrating that F-actin does not bind or binds very weakly either to the 140-kDa MBS-G-actin−S1 complex or to the 180-kDa complex.

Bettache et al. (1992) reported that the 140-kDa MBS-G-actin−S1 complex was suppressed by blocking Cys707-(SH1) in S1. Figure 9 shows the suppression of the 140-kDa complex by blocking SH1 in S1 with IAEDANS. The cross-linking between MBS-G-actin and SH1-modified S1 in the presence of ATP produced the 180-kDa band but not the 140-kDa band. A fluorescent 140-kDa band appeared together with a fluorescent 180-kDa band when MBS-G-actin was cross-linked to S1 which had been fluorescently labeled at the N-terminal 27-kDa fragment with 9-anthroylnitrile (data not shown). These results confirmed the previous report of Bettache et al. (1992) and suggested that the 140-kDa complex is produced by crosslinking of a free

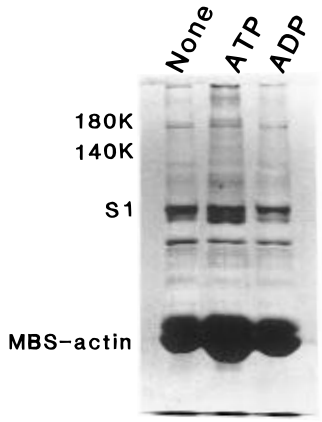

FIGURE 10: Chemical cross-linking of MBS-F-actin to S1 in the presence of ATP and ADP. MBS-F-actin was obtained by phalloidin-induced polymerization of MBS-G-actin (Miki & Hozumi, 1991). Reactive MBS-F-actin (10-20 μM actin monomer) was incubated with S1 (1 μM) for 40 min at 20 °C in the presence of MgATP (center lane) and MgADP (right lane). As a control, MgAMP was also added (left). Each 10 min, Mg-nucleotide (3 mM) was added 4 times. Other conditions were as in Figure 7.

maleimide group of MBS-actin to an SH1 thiol of S1 in the presence of ATP or ADP.

MBS-G-actin is polymerized to MBS-F-actin in the presence of phalloidin and salts (Miki & Hozumi, 1991). As reported by Bettache et al. (1992), MBS-F-actin was cross-linked to S1, producing an 180-kDa band apparently the same as that from MBS-G-actin and S1 (Figure 10, left lane). In the presence of ATP, MBS-F-actin and S1 produced 140- and 180-kDa bands as in the case of MBS-G-actin (Figure 10, center lane). However, the 140-kDa band became very weak when the S1 concentration was high enough to consume up ATP (data not shown). In contrast to MBS-G-actin, the 140-kDa band did not appear from MBS-F-actin and S1 in the presence of ADP (Figure 10, right lane). As in the case of MBS-G-actin, the cross-linking between SH1-modified S1 and MBS-F-actin produced only the 180-kDa band but not the 140-kDa band in the presence of ATP (data not shown). These results show that two 140- and 180-kDa complexes are very similar between MBS-G-actin−S1 and MBS-F-actin−S1 systems.

DISCUSSION

There are several advantages in studying stable actin monomers. One of them is to determine the number and location of actin-binding sites on S1. G-Actin whose polymerization had been inhibited by chemical modification (MBS or pyridoxal phosphate) retains the ability to bind to myosin heads and dissociate in the presence of ATP (Bettache et al., 1989; Arata, 1991; Valentin-Ranc et al., 1991). Two G-actin molecules binds to a myosin head (Arata, 1991; Valentin-Ranc et al., 1991). On the other hand, Chaussepied and his colleagues found that S1 with a light chain 3 forms only a 1:1 monomeric complex with G-actin at low ionic strength (Chaussepied & Kasprzak, 1989a,b; Lheureux et al., 1993). The second binding may stabilize a dimer of modified actins on S1, because the modified actins tend to polymerize at high salt and protein concentrations or by phalloidin (Bettache et al., 1990; Miki & Hozumi, 1991; Combeau & Carlier, 1992). In fact, S1 formed only a 1:1 complex with G-actin in which polymerization had been fully abolished by chemical modification (Arata, 1995). In the present study, we have examined the structural nature of two MBS-G-actin binding sites and the effect of ATP by tryptic digestion and chemical cross-linking.

MBS-G-actin protected the 27-kDa/50-kDa junction and also the 50-kDa/20-kDa junction weakly at an actin:S1 molar ratio of 1 (Figures 2 and 3). From the dependence on actin concentration of the protection of the 27-kDa/50-kDa junction, the dissociation constant of the 1:1 MBS-G-actin−S1 complex was determined to be $(1-2) \times 10^{-6}$ M. The affinity may be reduced by MBS modification as compared to those ($<10^{-7}$ M) with native G-actin (Lheureux & Chaussepied, 1995). It is unlikely that this reduced affinity is due to protein denaturation, because MBS-G-actin polymerizes to F-actin in the presence of phalloidin and activates the myosin ATPase (Miki & Hozumi, 1991; unpublished observation).

At the actin:S1 molar ratio of >2, protection of the 50-kDa/20-kDa junction is strengthened (Figures 2 and 3). This suggests that the additional binding of MBS-G-actin to the second sites of S1 strengthens the protection of the 50-kDa/20-kDa junction. In fact, the actual binding of MBS-G-actin to S1 is represented as the linear combination of the extents of strong protection of the 27-kDa/50-kDa and 50-kDa/20-kDa junctions (Figure 4). The cooperative binding for the second binding is well described by the sequential binding model (Valentin-Ranc et al., 1991): S1 + MBS-G-actin $\rightleftarrows$ S1−MBS-G-actin + MBS-G-actin $\rightleftarrows$ S1−$(\text{MBS-G-actin})_2$. This strongly supports the idea that two monomeric G-actin molecules bind to two different binding sites of S1 with different affinities involving protection of two tryptic junctions (Arata, 1991; Valentin-Ranc et al., 1991). However, this sequential model implies that actin−actin interactions occur in the ternary S1−$(\text{MBS-G-actin})_2$ complex. The actin−actin interactions on S1 may occur indirectly (through conformational changes transmitted between two sites) and/or occur very weakly in the dimer, because one of two MBS-G-actins bound to S1 is easily replaced by cross-linked actin dimer (Arata, 1991). From the dependence on actin concentration of the strong protection of the 20-kDa/50-kDa junction, the dissociation constant of S1−$(\text{MBS-G-actin})_2$ at the second site was determined to be $(4-5) \times 10^{-6}$ M.

In the presence of ATP, the protection of both 27-kDa/50-kDa and 50-kDa/20-kDa junctions needs much higher concentrations of MBS-G-actin (Figures 1 and 3). ATP perturbs both binding sites. The dissociation constants determined from the protection extents are $(2-3) \times 10^{-5}$ M, which is 10−30-fold weaker than in the absence of ATP. ADP appears to cause a small effect.

F-actin also protects both junctions from tryptic digestion in the absence and presence of ATP at low ionic strength (Figure 5), suggesting that the structures of two junctions are influenced by physiological F-actin−S1 binding. In the absence of ATP, only the 50-kDa/20-kDa junction of S1 was protected strongly from trypsin cleavage at low actin:S1 molar ratios (when S1 is in excess), suggesting a 1:1 stoichiometry. However, at high molar ratios of >2 (when actin is in excess), both 27-kDa/50-kDa and 50-kDa/20-kDa junctions were protected strongly, suggesting that S1 binds to two actin protomers (Andreeva et al., 1993).

The cross-linking data more directly showed that the different cross-linking sites are involved in making contact with actin at the first and second binding sites. EDC cross-linking between monomeric actin and S1 produces the doublet bands, and the 175-kDa band was much more

abundant than the 185-kDa band (Bettache et al., 1989; Hozumi, 1992; Combeau et al., 1992; Lheureux & Chaussepied, 1995). We also found that the 175-kDa band appears exclusively at the molar ratio of 1 (Figure 6), suggesting that N-terminal amino acids 1−12 of MBS-G-actin are EDC-cross-linked to the 20-kDa domain of S1 at the first site when the S1−MBS-G-actin complex forms (Sutoh, 1983). There appear 185-kDa and 210-kDa products (Figure 6) corresponding to the complex at the second site when the S1−$(MBS\text{-}G\text{-}actin)_2$ complex forms at ratios >2. However, we cannot exclude the possibility that the 185- and 210-kDa complexes are produced by the binding of the first actin and S1 with their interface stabilized by the second actin binding. The 185-kDa product is due to a cross-link between N-terminal amino acids 1−12 of actin and the 50-kDa domain of S1 (Sutoh, 1983). We provide no evidence of what the 210-kDa product is. This product may be the same as those generated by the cross-links between the N-terminal part (residues 1−12 or 40−113) of actin and the 50-kDa domain of S1 (Bertrand et al., 1988; Combeau et al., 1992; Bonafe & Chaussepied, 1995).

The two-site model for acto−S1 binding has also been proposed from the binding studies and chemical cross-linking studies showing that the mode of binding depends on the molar ratio of actin to S1 (Valentin-Ranc et al., 1991; Arata, 1991; Andreev & Borejdo, 1991; Yamamoto, 1986, 1990; Combeau et al., 1992). Andreeva et al. (1993) and later Bonafe and Chaussepied (1995) directly demonstrated that the 265-kDa complex was produced by EDC cross-linking of F-actin and S1 at higher molar ratios >2 and contained two actins and one S1. They concluded that a single S1 is cross-linked to both N-termini of the first and second actin protomers through its 20- and 50-kDa domains, respectively. The N-terminus in subdomain 1 of each actin is thought to be cross-linked to the residues of loops 626−647 and 567−578 in S1 heavy chain (Sutoh, 1983; Andreeva et al., 1993; Bonafe & Chaussepied, 1995). Although the loops are highly mobile and cannot be seen, the center-to-center distance between two junctions extruding these loops would give 5 nm and may be enough to span two actin monomers (Rayment et al., 1993a). A recent model of F-acto−S1 structure suggests that a single S1 molecule can interact with two adjacent actin protomers at low actin:S1 molar ratios (Milligan et al., 1990; Rayment et al., 1993b). The second binding becomes stronger or available only at higher ratios (Andreev & Borejdo, 1995). The present results also showed that two actins are complexed at higher ratios.

Residues 48−67 in actin subdomain 2 (cross-linked to 50-kDa domain of S1) are also responsible for the 180-kDa MBS cross-linked complex (Bertrand et al., 1994). This cross-linked complex is produced when the first MBS-actin binds to S1 at the actin:S1 molar ratio of 1 (Figure 7) or when the MBS-actin complexed with DNase I binds to S1 (Bettache et al., 1989). Thus two domains (1 and 2) seem to interact with S1 and produce MBS and EDC cross-links. However, Lheureux and Chaussepied (1995) reported that S1 made an amino group-directed cross-link with subdomain 2 of F-actin but did not cross-link with subdomain 2 of G-actin complexed with DNase I. This discrepancy remains unclear. One possibility is that the first binding site spreads over two domains of actin monomer, although it is inconsistent with the recent 3D model of Rayment et al. (1993b). Bertrand et al. (1994) postulated a possibility that S1 binds to a small amount of dimeric form of MBS-actin in equilibrium with monomeric form, making an MBS cross-link with subdomain 2 as with F-actin. It is also possible that at the 1:1 molar ratio MBS-actin as a monomer binds mainly to the first site but partly to the second site, making only MBS cross-link through its subdomain 2. (EDC cross-linking at the second site occurs only when two actins bind.) MBS may cross-link a completely different site than EDC.

In the presence of ATP or ADP, a new MBS cross-linked 140-kDa complex between MBS-G-actin and S1 was generated together with the 180-kDa complex (Figures 7 and 8). Like the 180-kDa complex, the 140-kDa complex did not bind to native F-actin (Figure 8). The 180-kDa complex is produced between actin and the 50-kDa domain of S1 (Bettache et al., 1989). The 140-kDa complex is essentially the same as that discovered by Bettache et al. (1992), because the 140-kDa complex was suppressed by blocking Cys707 (SH1) of S1 (Figure 9). They concluded that SH1 of S1 is specifically cross-linked to MBS-actin in their buffer (containing ADP). On the other hand, EDC-cross-linked 175−185-kDa complexes were suppressed in the presence of ATP or ADP, although ATP had a much greater effect than ADP. These data suggest that the binding site in MBS-G-actin−S1 complex is shifting between the Cys707 (MBS) and the rigor sites on 50-kDa (MBS) and 20−50-kDa (EDC) domains.

MBS-G-actin is polymerized to normal F-actin in the presence of phalloidin (Miki & Hozumi, 1991). In the presence of ATP, 140- and 180-kDa MBS complexes are produced between MBS-F-actin and S1 as observed when MBS-G-actin and S1 are cross-linked in the presence of ATP or ADP (Figure 10). However, there appears to be no 140-kDa complex when MBS-F-actin and S1 are cross-linked in the presence of ADP. These results suggest that the surfaces between actin and S1 are the same or overlapped between F- and G-acto−S1 complexes in the absence and presence of ATP and that the effect of ADP on the binding site(s) is considerably different between these complexes. The shifting of binding site in F-actin−S1 complex may also occur between Cys707 and the rigor sites on S1 in the presence of ATP but not ADP. It has been reported that Cys707 is 5−6 nm away from the actin-binding site in the absence of ATP (Rayment et al., 1993b; Tokunaga et al., 1987; Arata, 1986). Thus, the ATP-induced shifting may be considerably large and play an important role in muscle contraction.

These monomeric MBS-actin−S1 complexes may represent a useful model system for studying the three-dimensional structure of actin-bound myosin head during ATP hydrolysis. The electron microscopic examination is now in progress in my laboratory to determine the topography of the actin binding region on the head decorated by an MBS-actin (Arata, 1993, 1995).

REFERENCES

Andreev, O. A., & Borejdo, J. (1991) *Biochem. Biophys. Res. Commun. 177*, 350−356.
Andreev, O. A., & Borejdo, J. (1995) *Biochemistry 34*, 14829−14833.
Andreev, O. A., Andreeva, A. L., & Borejdo, J. (1993) *Biophys. J. 65*, 1027−1038.
Andreeva, A. L., Andreev, O. A., & Borejdo, J. (1993) *Biochemistry 32*, 13956−13960.
Arata, T. (1986) *J. Mol. Biol. 191*, 107−116.
Arata, T. (1991) *J. Biochem. (Tokyo) 109*, 335−340.

Arata, T. (1993) *Adv. Exp. Med. Biol. 332*, 790−792.
Arata, T. (1995) *Biophys. J. 68*, 325s.
Bertrand, R., Chaussepied, P., Kassab, R., Boyer, M., Roustan, C., & Benyamin, Y. (1988) *Biochemistry 27*, 5723−5736.
Bertrand, R., Derancourt, J., & Kassab, R. (1994) *FEBS Lett. 345*, 113−119.
Bettache, N., Bertrand, R., & Kassab, R. (1989) *Proc. Natl. Acad. Sci. U.S.A. 86*, 6028−6032.
Bettache, N., Bertrand, R., & Kassab, R. (1990) *Biochemistry 29*, 9085−9091.
Bettache, N., Bertrand, R., & Kassab, R. (1992) *Biochemistry 31*, 389−395.
Bonafe, N., & Chaussepied, P. (1995) *Biophys. J. 68*, 35s−43s.
Bradford, M. M. (1976) *Anal. Biochem. 72*, 248−254.
Chaussepied, P., & Kasprzak, A. A. (1989a) *Nature 342*, 950−953.
Chaussepied, P., & Kasprzak, A. A. (1989b) *J. Biol. Chem. 264*, 20752−20759.
Combeau, C., & Carlier, M.-F. (1992) *Biochemistry 31*, 300−309.
Combeau, C., Didry, D., & Carlier, M.-F. (1992) *J. Biol. Chem. 267*, 14038−14046.
dos Remedios, C. G., & Moens, P. D. J. (1995) *Biochim. Biophys. Acta 1228*, 99−124.
Heintz, D., & Faulstich, H. (1996) *Biochemistry 35*, 258−265.
Hiratsuka, T. (1989) *J. Biol. Chem. 264*, 18188−18194.
Hozumi, T. (1983) *Biochemistry 22*, 799−804.
Hozumi, T. (1992) *Biochemistry 31*, 10070−10073.
Huxley, A. F., & Niedergerke, R. (1954) *Nature 173*, 971−973.
Huxley, H. E., & Hanson, J. (1954) *Nature 173*, 973−976.
Laemmli, U. K. (1970) *Nature 227*, 680−685.
Lheureux, K., & Chaussepied, P. (1995) *Biochemistry 34*, 11435−11444.
Lheureux, K., & Forne, T., Chaussepied, P. (1993) *Biochemistry 32*, 10005−10014.
Miki, M., & Hozumi, T. (1991) *Biochemistry 30*, 5625−5630.
Milligan, R. A., Whittacker, M., & Safer, D. (1990) *Nature 348*, 217−221.
Mornet, D., Pantel, P., Audemard, E., & Kassab, R. (1979) *Biochem. Biophys. Res. Commun. 89*, 925−932.
Mornet, D., Bertrand, R., Audemard, E., & Kassab, R. (1981) *Nature 292*, 301−306.
Muhlrad, A., & Hozumi, T. (1982) *Proc. Natl. Acad. Sci. U.S.A. 79*, 958−962.
Perry, S. V. (1955) *Methods Enzymol. 2*, 583−588.
Rayment, I., Rypniewski, W. R., Schmidt-Base, K., Smith, R., Tomchick, D. R., Benning, M. M., Winkelmann, D. A., Wesenberg, G., & Holden, H. M. (1993a) *Science 261*, 50−58.
Rayment, I., Holden, H. M., Whittacker, M., Yohn, C. B., Lorenz, M., Holmes, K. C., & Milligan, R. A. (1993b) *Science 261*, 58−65.
Raynard, A. M., Hass, L. E., Jacobsen, D. D., & Boyer, P. D. (1961) *J. Biol. Chem. 236*, 2277−2288.
Sutoh, K. (1983) *Biochemistry 22*, 1579−1585.
Tokunaga, M., Sutoh, K., Toyoshima, C., & Wakabayashi, T. (1987) *Nature 329*, 635−638.
Valentin-Ranc, C., Combeau, C., Pantaloni, D., & Carlier, M.-F. (1991) *J. Biol. Chem. 266*, 17872−17879.
Weeds, A. G., & Taylor, R. S. (1975) *Nature 257*, 54−56.
Yamamoto, K. (1989) *Biochemistry 28*, 5573−5577.
Yamamoto, K. (1990) *Biochemistry 29*, 844−848.

BI960803S